

# Supplementary Information for Robustly Nano-tailored Honeycomb Structure for High- throughput Antireflection Polymer Film

Kiwoon Choi<sup>†</sup>, Sung Ho Park<sup>†</sup>, Young Min Song<sup>§</sup>, Chongdu Cho<sup>‡</sup>, Han Sup Lee<sup>†,\*</sup>

<sup>†</sup>Department of Advanced Fiber Engineering, and <sup>‡</sup>Department of Mechanical Engineering, Inha University, 253 Young-hyun-dong, Nam-gu, Incheon, 402-751, Republic of Korea

<sup>§</sup>Department of Materials Science and Engineering, University of Illinois at Urbana Champaign, Urbana, Illinois 61801, USA

## 1. Materials

### 1-1. PMMA

Various inorganic optical components have been replaced with plastic materials owing to their good mechanical and optical properties, easy and fast processibility, and lightness. Poly(methyl methacrylate) (PMMA) has been used extensively as a transparent polymer for a range of optics and optoelectronics applications. Since the glass transition temperature ( $T_g$ ) of PMMA is relatively low, it is used widely for roll-to-roll processible thermal nanoimprint lithography (RTNIL) processes during which the molding and demolding steps are carried out at temperatures lower and higher than the  $T_g$  of PMMA, respectively.<sup>1</sup> In this study, a high performance AR product was fabricated based on a negative antireflective structure (N-ARS) with PMMA.

## 2. Sample Preparation.

### 2-1. Original mold fabrication with the multistep anodization and etching method

Highly pure aluminum discs (99.999%, Goodfellow), 50 mm in diameter and 0.5 mm in thickness, were cleaned with acetone in an ultrasonic bath. The disc was then immersed for 2 min at 60 °C in a mixture containing HF/HNO<sub>3</sub>/HCl/H<sub>2</sub>O at a volume ratio of 1:10:20:69 to remove the impurities from the surface. After the cleaning with deionized (DI) water, the Al discs were annealed for 3 hours at 500 °C in N<sub>2</sub> to obtain large single-crystalline grains. The

domain size of the self-ordered porous alumina increased with increasing grain size. To reduce the surface roughness, electropolishing was performed at 20 V for 3 min in a mixture consisting of 1/4 HClO<sub>4</sub> and 3/4 C<sub>2</sub>H<sub>5</sub>OH. During this process, the stirring rate was adjusted to maintain the current at a level of approximately 1.0 mA/mm<sup>2</sup>. Electropolishing is a prerequisite for the formation of self-ordered porous alumina with a large domain size. After the pretreatment, the initial anodization was performed by applying 80 V at -10 °C in 0.1 M (COOH)<sub>2</sub> (mixture consisting of 3/5 H<sub>2</sub>O and 2/5 C<sub>2</sub>H<sub>5</sub>OH) for more than 1 day. Performing the anodization process in a mixture of water and ethanol to lower the freezing temperature of the electrolyte used allowed the anodization process to be carried out reproducibly without the electrical breakdown caused by local heating.<sup>2</sup> The initial pore arrangement was highly irregular because pores were created randomly on the surface. On the other hand, self-organization occurred due to the repulsive forces of the neighboring pores during the long anodization time. As a result, hexagonally packed arrays were obtained at the interface of the porous alumina layer and aluminum substrate. The porous alumina film was then dissolved selectively in a chromic acid solution (100 mL of an aquatic solution containing 1.8 g CrO<sub>3</sub> and 7.1 g H<sub>3</sub>PO<sub>4</sub>) at 60 °C for 12 hours. Any patterns that were replicas of the hexagonal pore array were preserved on a fresh aluminum surface. The hexagonal pattern enabled pores with high regularity to be prepared during a subsequent multistep anodization process under the same conditions as the previous anodization process.<sup>3</sup> Chemical etching in a multistep anodization process was performed at 30 °C in 0.3 M of (COOH)<sub>2</sub> without any potential difference between the anode and cathode. During the multistep anodization and etching process, the diameter of the pores at each sublayer could be controlled precisely by changing

Type	Process	Process time					Total
		1 <sup>st</sup> Step	2 <sup>nd</sup> Step	3 <sup>rd</sup> Step	4 <sup>th</sup> Step	5 <sup>th</sup> Step	
N-ARS	Anodization	28'	28'	28'	28'	28'	2" 20'
	Etching	67"	77"	88"	115"	183"	530"
P-ARS	Anodization	28'	28'	28'	28'	28'	2" 20'
	Etching	63"	73"	87"	115"	200"	538"

(" : min, ' : second)

**Table S1.** Process times for each anodization and etching step during the multistep anodization process to prepare AAO with tapered pores.

the anodization and etching times under the conditions described in **Table S1**. Two different anodized aluminum oxide (AAO) templates with slightly different surface profiles could be fabricated to ensure an identical refractive index (RI) profile inside the interphase layers of the N-ARS and P-ARS PMMA films.<sup>4</sup>

## 2-2. Fabrication of a PMMA AR film with P-ARS using the vacuum-assisted template wetting method

A vacuum-assisted template wetting method was used to prepare the P-ARS film using the AAO original mold because it was impossible to apply pressure-driven thermal nanoimprint lithography to fabricate a PMMA AR film with P-ARS on its surface due to the closed-channel characteristics of pores in AAO. **Figure S1** shows a schematic diagram of the vacuum-assisted template wetting method used in this study to fabricate the P-ARS AR film. Inside the vacuum chamber, the flat PMMA film was placed on the AAO templates. After maintaining the pores under vacuum, the PMMA film and AAO template were heated to 150 °C and the AAO templates were pressed against the molten PMMA to seal the pores under vacuum. The pores in the AAO template could be infiltrated with molten PMMA by purging the vacuum chamber while maintaining the PMMA under pressure. After cooling, the remaining aluminum layer was dissolved in a copper solution ( $\text{CuCl}_2 \cdot \text{H}_2\text{O}$  6.8 g + 37% HCl 200 mL + distilled water 200 mL) and the alumina layer was removed in the chromic acid



**Figure S1.** Schematic diagram of the vacuum-assisted template wetting method for the fabrication of P-ARSs on a PMMA film surface. **1)** The PMMA film was deposited on an AAO template with nanopores on one surface and placed in a vacuum. **2)** The entire set was heated to a temperature higher than the glass transition temperature of PMMA. **3)** The heated PMMA film was pressed against the AAO template to seal the nanopores, and the vacuum was released so that the nanopores in AAO could be filled with molten PMMA as a result of the difference in surface tension between the alumina wall and polymer; this process was facilitated by the difference in pressure between inside and outside the pores. **4)** When the pores were filled completely, the entire set was cooled to room temperature. **5)** The AAO template was dissolved chemically so that the PMMA film contained P-ARSs on a single surface.



tailored by applying a multistep anodization and etching method, the schematic process of which is illustrated in **Figure S2**. As shown in **Figure S2**, the 5-step anodization and etching method will eventually produce 5-sublayer pores consisting of the first-sublayer, second-sublayer, third-sublayer, etc. First, the initial diameter and depth of the pores in the first sublayer were determined during the first step anodization and etching processes according to Equations S1 and S2. When the second step anodization process was applied, the pores in the second sublayer were formed. Upon the second step etching process, the pore diameters in the first and second sublayers were increased according to Equation S2. By continuing this process 5 times, it was possible to prepare pores in AAO consisting of five sublayers with different diameters, as shown in the right side of **Figure S2**. The overall pore depth ( $L$ ) and

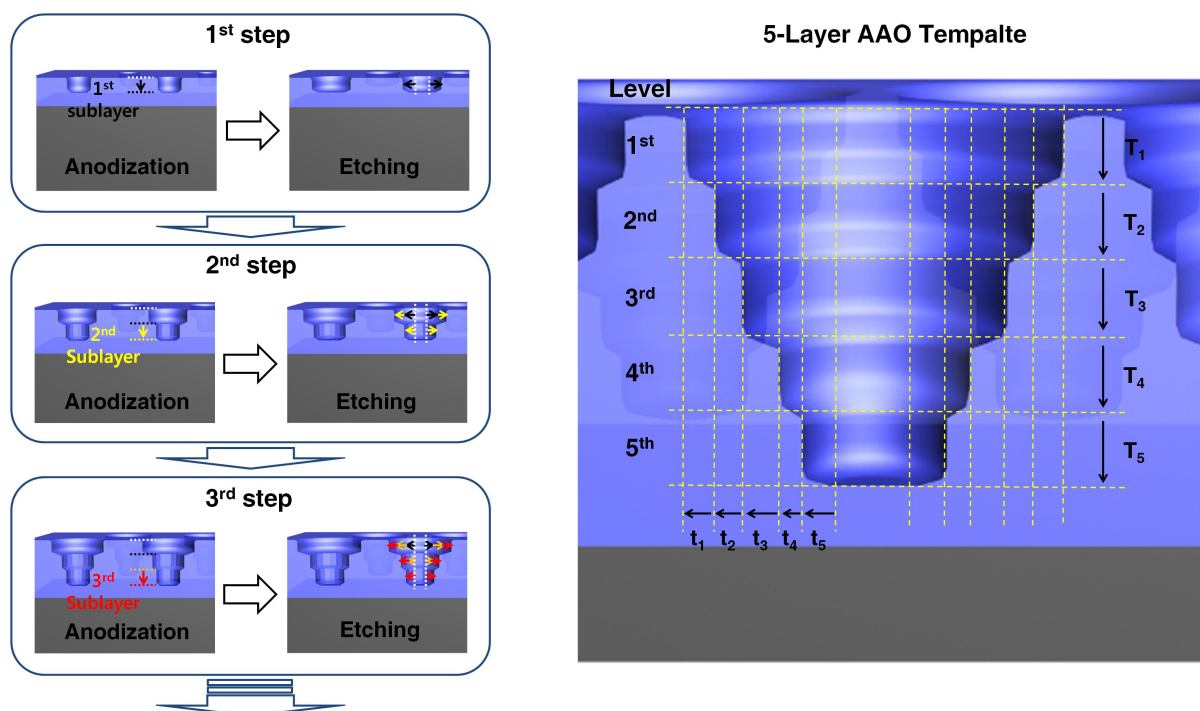


**Figure S2.** Pore shape changes during multistep anodization process (left) and the eventual pore shape after the 5-step anodization process (right). During the first anodization step, pores in the first sublayer formed and their diameters were increased during the subsequent etching step. During the second anodization step, the pores in the second sublayer were formed. The diameters of the pores in the first and second sublayers were increased further during the second etching step. During the third anodization step, the pores in the third sublayer were formed. The diameters of the pores in the first, second and third sublayers were increased further during the third etching step. Pores with the five sublayer shapes shown in the right hand side can be formed by continuing this process until the fifth step.

eventual diameter of the pores in the first sublayer were determined by the total anodization time ( $T$ ) and total etching time ( $t$ ) according to Equations S1 and S2, respectively. The depth of each sublayer ( $L_i$ ) can be determined by the corresponding anodization time ( $T_i$ ), and the diameter of each sublayer ( $D_i$ ) is a function of the accumulated etching time ( $t_i + t_{i+1} + \dots + t_5$ ). By carefully controlling the anodization time ( $T_i$ ) and etching time ( $t_i$ ) for each sublayer, it was possible to tailor the dimensions of the pores in each sublayer in AAO to eventually obtain desired RI profile of the ARS layer.

### 3-2. The importance of the ARS period

For an ARS surface, it is essential that the period ( $d$ ) of the ARSs be sufficiently small so the array cannot be resolved by the incident light ( $d < \lambda/n$ ).<sup>6</sup> Good AR performance over a broad wavelength range can be achieved with the ARS array of a smaller period. In preliminary work (data not shown) with the ARS of a 300 nm period, a rapid decrease in transmittance was observed over the 400-500 nm wavelength range, which might be due to higher order diffraction.<sup>7</sup> The mechanical stability of positive structures can be decreased significantly if the period is reduced to well below 200 nm to lead eventually to a high aspect ratio of positive structures on the PI mold surface. It is also almost impossible to achieve clean release of a N-ARS film probably due to the increased contact area between the imprinted PMMA film and PI roller mold. Therefore, a 200 nm period was used for N-ARS fabrication, which is the maximum value to ensure high AR performance over the entire visible wavelength range (400~800 nm) and possibly the optimum value to achieve high mechanical stability of positive structures on a PI roller mold while maintaining clear mold release during the RTNIL process.

### References

1. H. Schiff, *J. Vac. Sci. Technol. B* 2008, **26**, 458.
2. Y. Li, M. Zheng, L. Ma and W. Shen, *Nanotechnology* 2006, **17**, 5101.
3. H. Masuda and K. Fukuda, *Science* 1995, **268**, 1466-1468.
4. K. Choi, S. H. Park, Y. M. Song, Y. T. Lee, C. K. Hwangbo, H. Yang and H. S. Lee, *Adv. Mater.* 2010, **22**, 3713.
5. K. Nielsch, J. Choi, K. Schwirn, R. B. Wehrspohn and U. Gosele, *Nano Lett.* 2002, **2**, 677.

6. Y. Li, J. Zhang and B. Yang, *Nano Today* 2010, **5**, 117-127.

7. Y. M. Song, H. J. Choi, J. S. Yu and Y. T. Lee, *Opt. Express* 2010, **18**, 13063.